Numerical analysis of vectorial two-beam coupling in photorefractive materials

Vittorio M. N. Passaro and Daniele Marseglia
Optoelectronics Laboratory, Dipartimento di Elettrotecnica ed Elettronica
Politecnico di Bari, Via Edoardo Orabona 4 – 70125 Bari, Italy
passaro@poliba.it, maddanny@libero.it

Abstract: A numerical model is presented for the analysis of vectorial two-beam coupling in photorefractive materials. A powerful software tool has been developed for design purposes. For Fe,Ce-doped lithium niobate crystals, conversion efficiency and signal gain dependences on experimental parameters and beam polarization have been found. The good accuracy of the model has been demonstrated by comparisons with experimentally measured parameters.

OCIS Codes: (090.2900) Holographic recording materials; (130.3730) Lithium niobate; (160.5320) Photorefractive materials; (210.2860) Holographic and volume memories.

References and links

1. B. Fischer, M. Cronin-Golomb, J. O. White, A. Yariv, "Nonlinear vectorial two-beam coupling and forward four-wave mixing in photorefractive materials," Opt. Letters **11**, 239-241 (1986).
2. J. Feinberg, K. R. MacDonald, "Phase-conjugate mirrors and resonators with photorefractive materials," in *Photorefractive Materials and their applications II*, 151-203 (Springer-Verlag, Berlin, 1988).
3. C. Yang, Y. Zhao, R. Wang, M. Li, "Studies of photorefractive crystals of double-doped Ce,Fe:$LiNbO_3$," Opt. Commun. **175**, 247-252 (2000).
4. J. O. White, S. K. Kwong, M. Cronin-Golomb, B. Fischer, A. Yariv, "Wave propagation in photorefractive media," in *Photorefractive Materials and their applications II*, 101-150 (Springer-Verlag, Berlin, 1988).
5. P. Gunter, J. P. Huignard, "Photorefractive effects and materials," in *Photorefractive Materials and their applications I*, 7-74 (Springer-Verlag, Berlin, 1988).

1. Introduction

Photorefractive crystals, making possible an efficient steady-state energy transfer from a reference beam into an object beam (phase-conjugate), have attracted particular attention as media for dynamic recording and transformation of light beams. Therefore, photorefractive crystals are considered as excellent non-linear media for implementing phase conjugate mirrors, wave-front correction and real-time interferometry. They are also viewed as parametric gain media for a new type of optical oscillator. Moreover, the relevant light wave amplitude changes induced by them result in energy exchange that can be used for image amplification and real-time processing. Therefore, it is important to develop a full vectorial model of two-beam coupling in these photorefractive crystals.

2. Mathematical model

Two laser beams writing a holographic grating in a photorefractive medium are coupled nonlinearly to each other. The nonlinear coupled-wave equations which describe this physical mechanism have been analytically solved in literature either for a scalar case, i.e. two beams with the same polarization, or for a vectorial case, i.e. two beams with arbitrary polarization, but under the heavy approximation of neglecting the cross-coupling effect [1].

Figure 1 shows the vectorial two-beam coupling geometry analysed in our model. Two beams (the signal beam and reference one) propagate in the crystal (width d). Their vectorial field amplitudes are represented by two orthogonal components, (A_1, A_2) and (A_3, A_4) respectively. We note that A_1 and A_4 are not parallel (with arbitrary mismatch angle ϕ_{14}) and

#1761 - $15.00 US Received October 21, 2002; Revised November 15, 2002

observe that the angles formed by the beam propagation directions with the optic axis are in general different, i.e., ϑ_1 and ϑ_2. Without any lack in generality, the optic axis coincident with the z axis is assumed in Fig. 1 as a particular case of our model.

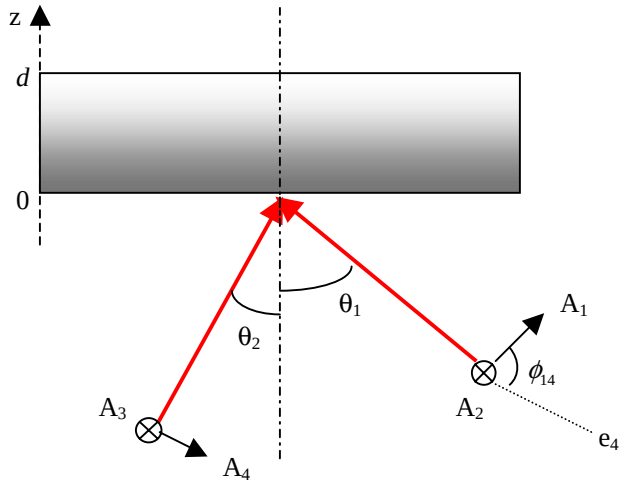

Fig. 1. Vectorial two-beam coupling geometry.

If we assume the same wavelength (i.e. the same source) for both incident waves and the same coupling constants (real) for both the polarizations [1], under the hypothesis of moderate power levels [2] the coupled-wave equation system describing the amplitude changes inside the grating can be written as follows:

$$\begin{cases} \dfrac{dA_1}{dz} = -\gamma_I g A_4 - \gamma_{II} g A_3 - \alpha A_1 \\ \dfrac{dA_2}{dz} = -\gamma_I g A_3 - \gamma_{II} g A_4 - \alpha A_2 \\ \dfrac{dA_3^*}{dz} = -\gamma_I g A_2^* - \gamma_{II} g A_1^* - \alpha A_3^* \\ \dfrac{dA_4^*}{dz} = -\gamma_I g A_1^* - \gamma_{II} g A_2^* - \alpha A_4^* \end{cases} \tag{1}$$

where the α is linear absorption coefficient, $g = (A_1 A_4^* + A_2 A_3^*)/I_0$ and $I_0 = \sum_i I_i = \sum_i |A_i|^2 = \sum_i A_i A_i^*$.

In Eq. (1), γ_I and γ_{II} are the coupling coefficients between homologous field components (i.e. A_1 and A_4 or A_2 and A_3) and not homologous ones (i.e. A_1 and A_3 or A_2 and A_4), respectively. The above equations are normalized with respect to the total intensity, I_0. Since the field components are complex (the asterisk designating the complex conjugate), we can write them as:

$A_i = \mathrm{Re}\{A_i\} + j\,\mathrm{Im}\{A_i\}$ i = 1, 2, 3, 4

$g = \mathrm{Re}\{g\} + j\,\mathrm{Im}\{g\} =$

#1761 - $15.00 US
Received October 21, 2002; Revised November 15, 2002

$$= \left(\mathrm{Re}\{A_1\}\mathrm{Re}\{A_4\} + \mathrm{Im}\{A_1\}\mathrm{Im}\{A_4\} + \mathrm{Re}\{A_2\}\mathrm{Re}\{A_3\} + \mathrm{Im}\{A_2\}\mathrm{Im}\{A_3\} \right) +$$
$$+ j\left(\mathrm{Re}\{A_4\}\mathrm{Im}\{A_1\} - \mathrm{Re}\{A_1\}\mathrm{Im}\{A_4\} + \mathrm{Re}\{A_3\}\mathrm{Im}\{A_2\} - \mathrm{Re}\{A_2\}\mathrm{Im}\{A_3\} \right)$$

and, then, explicitly write the system (1) in terms of eight equations as a function of eight real unknowns, i.e. $\mathrm{Re}\{A_1\}$, $\mathrm{Re}\{A_2\}$, $\mathrm{Re}\{A_3\}$, $\mathrm{Re}\{A_4\}$, $\mathrm{Im}\{A_1\}$, $\mathrm{Im}\{A_2\}$, $\mathrm{Im}\{A_3\}$, $\mathrm{Im}\{A_4\}$. The linear absorption coefficient α depends on the incident wavelength, material and doping. Now, since the coupling coefficients depend on the geometry parameters, the grating vector amplitude, the dielectric ε and the electro-optic r tensors of the crystal, we use for γ_I, γ_{II} the general expression as in [2]:

$$\gamma_p = \frac{4\pi}{\lambda}\frac{k_B T}{q}\frac{r_{eff}}{n\cos\left[\frac{\vartheta_1 + \vartheta_2}{2}\right]} \cdot \frac{|\bar{K}|}{1 + \left(\frac{|\bar{K}|}{k_o}\right)^2} e_1 \varepsilon e_2^* \qquad p = I, II \tag{2}$$

where k_B is the Boltzmann constant, q is the electron charge, n is the substrate refractive index, $|\bar{K}|$ is the grating vector amplitude, e_1 and e_2 are the polarization vectors of the generic interacting components. Moreover, two important factors are present in Eq. (2), i.e. the Debye length k_o, and the effective electro-optic coefficient r_{eff}. The former has been evaluated by the following expression [3]:

$$k_0 = \sqrt{\frac{4\pi N_{eff} q^2}{\varepsilon_0 \varepsilon_{rK} k_B T}} \tag{3}$$

where

ε_0 = 8.85 10^{-12} [F/m] and $\varepsilon_{rK} = \dfrac{\bar{K} \cdot \varepsilon \bar{K}}{|\bar{K}|^2}$ (dimensionless dielectric constant along $\bar{K}$).

The parameter N_{eff} represents the effective density of photorefractive traps and its value, experimentally evaluated, depends on the doping process and wavelength. Moreover, the generic expression for r_{eff} is [2]:

$$r_{eff} = \frac{1}{n^4} e_1^* \cdot \left\{ \varepsilon \left[r \left(\frac{\bar{K}}{|\bar{K}|} \right) \right] \cdot \varepsilon \right\} \cdot e_2 \tag{4}$$

Of course, the values of the electro-optic components depend on the wavelength and, in general, even on the doping profile. Finally, we underline that the above analysis and the related expressions are valid in the absence of any applied electric field, either external or internal (photovoltaic). If they should present, instead, there should result in a significant increase of non linearity [4].

3. Numerical results

The developed software tool is a powerful instrument for design purposes due to its generality and versatility. It is based on the solution of the modified system (1) by a numerical routine, being the coupling constants evaluated as in Eq. (2). In the code, a large number of geometry and physical parameters can be selected, i.e. I_0, α, λ, T, n, ϑ_1, ϑ_2, ϕ_{14}, d, N_{eff}, ε and r, giving to our model the potential to predict the behaviour of the two-beam coupling mechanism occurring in several different experimental set-ups.

#1761 - $15.00 US Received October 21, 2002; Revised November 15, 2002

To point out some useful results, let us consider the real case of a Ce,Fe:$LiNbO_3$ crystal at room temperature (T=300 K), having width $d = 1mm$, $N_{eff} = 0.1 \cdot 10^{-15}$ cm^{-3} and $\alpha = 0.70$ cm^{-1} at the wavelength of 632.8 nm. This test case was experimentally investigated in Ref. [3]. We have assumed a mismatch angle between oblique directions $\phi_{14} = 10°$. The conversion efficiency η (defined as the power ratio between the object beam at the output and the reference beam at the input) has been numerically evaluated for different polarizations (i.e. both extraordinary beams with $n = n_e$, or both ordinary beams with $n = n_o$) as a function of the crossing angle ϑ_C, assuming in particular $\vartheta_1 = \vartheta_2 = \vartheta_C / 2$ (see Fig. 2). In the routine, the grating period Λ (and so the grating vector amplitude, $|\bar{K}| = 2\pi / \Lambda$) has been evaluated by the following expression [5]:

$$\Lambda = \frac{\lambda}{2n \sin(\vartheta_C / 2)} \tag{5}$$

since we are under the hypothesis of considering the same polarization for both the incident beams.

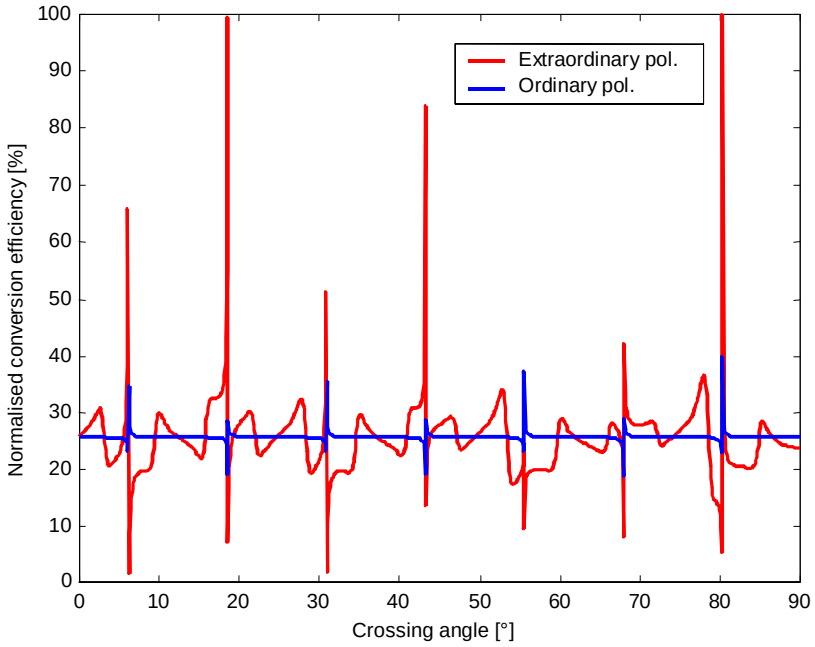

Fig. 2. Conversion efficiency dependence on crossing angle.

It is evident that the conversion efficiency remain around 26% for ordinary polarization (blue line), only one peak reaching 40% at 80.3°, while two high-efficiency main peaks can be detected for extraordinary polarization (red line), approaching 100% at 18.5° and 80.3°, respectively. The number of peaks in Fig. 2 are obtained when the Bragg condition is perfectly satisfied and the coupling coefficients are maximized, depending on the coupling geometry and beam polarization. For comparison purposes with more approximated approaches, the same simulation for extraordinary polarization has been carried out by

#1761 - $15.00 US
Received October 21, 2002; Revised November 15, 2002

neglecting the crossing coupling effect (i.e. $\gamma_{II} = 0$, green line in Fig. 3). We can note that the approximated method gives under-estimated results.

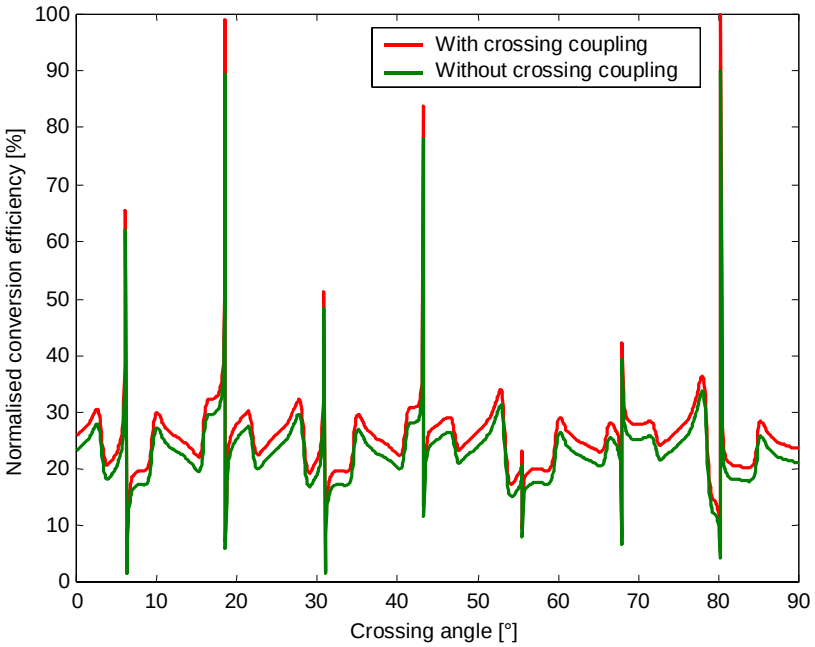

Fig. 3. Conversion efficiency dependence on crossing angle.

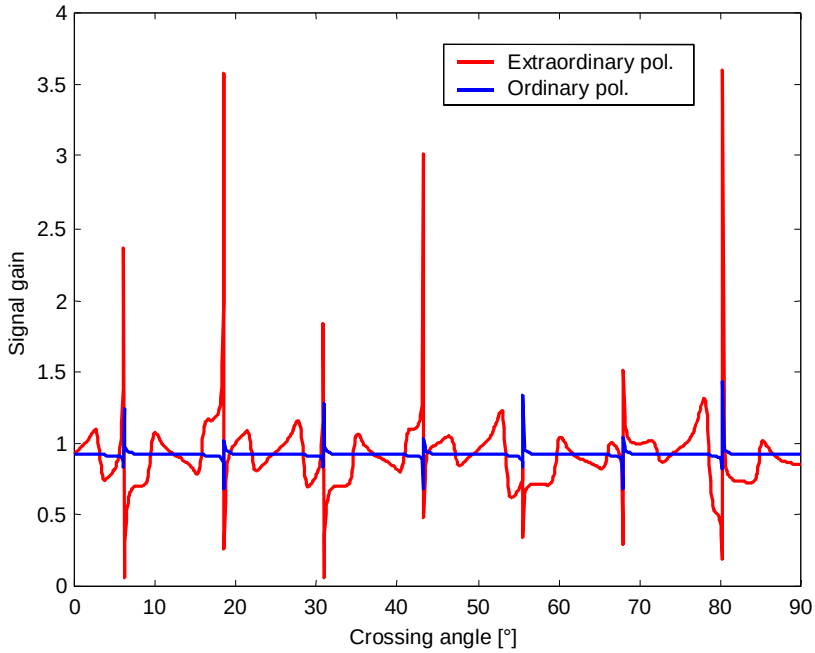

Fig. 4. Signal gain dependence on crossing angle.

#1761 - $15.00 US
Received October 21, 2002; Revised November 15, 2002

In the above conditions, we have also evaluated the relevant signal gain, as in Fig. 4, only for extraordinary polarization. It is clear that we can obtain a signal gain close to 3.5 at the crossing angles of 18.2° and 80.3°. These results can be useful for the design of photorefractivity-based optical amplifiers.

With the aim to show our software features, we consider now to be under the same experimental conditions as above and to change the oblique direction mismatch angle (o.d.m.a., or ϕ_{14}), in order to better match a real experimental condition. Figure 5 clearly shows the gain peaks around 80.3° and how the signal gain does not significantly change up to an o.d.m.a. of 45°, but it reduces from a factor around 3.5 to a factor around 2.5 at an o.d.m.a. of 90°. Thus, we have shown how critically the signal gain depends both on crossing angle and on the oblique directions mismatch angle.

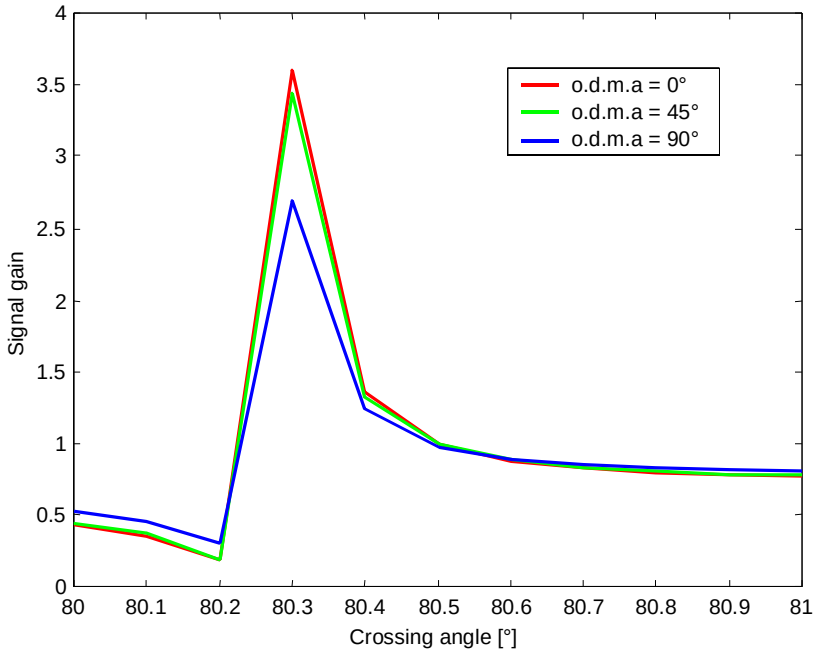

Fig. 5. Signal gain dependence on crossing angle.

To demonstrate the accuracy of our results and the model versatility, we have also carried out a number of simulations by assuming different experimental conditions. We have numerically evaluated the two-beam coupling gain coefficient, Γ_{num}, and then compared the results with respect to those experimentally found in Ref. [5] (i.e. Γ_{exp}), where a number of $LiNbO_3$ crystals with different Fe and Ce doping and process treatment were considered. The two-beam coupling gain coefficient has been defined as $\Gamma = \ln\left(I_S^{twm}/I_S\right)/L$ [3], where L is the beam interaction length (i.e. the thickness of the sample, d =1 mm), I_S^{twm} is the transmitted signal beam intensity when the coupling effect occurs and I_S is the transmitted signal beam intensity without any interaction, i.e. when only the linear absorption effect occurs.

The above approximated expression is valid when the pump beam intensity is much larger than the signal beam one. In our case this condition is satisfied if we consider a

Received October 21, 2002; Revised November 15, 2002

pump/signal intensity ratio of 750 for a normalised total intensity of 1mW/cm^2. The results of simulations and comparisons are summarized in Table I.

It is clear that a good agreement between the experimental and numerical values can be obtained by our model, showing a percentage relative error lower than 5% (see the last red column) under all the experimental conditions.

Table 1. Comparisons among experimental [3] and numerical values of two-beam coupling gain coefficient Γ.

$LiNbO_3$ Crystal doping	Treatment	λ [nm]	α [cm^{-1}]	ϑ_C [°]	N_{eff} [10^{15} cm^{-3}]	Γ_{exp} [cm^{-1}]	Γ_{num} [cm^{-1}]	e_r [%]
Ce	Reduction	488	3.6	9.0	0.2	**24.0**	**24.45**	**1.87**
Fe	Reduction	488	21.1	31.0	2.2	**36.4**	**37.32**	**2.52**
Ce, Fe	Reduction	488	21.2	36.0	2.9	**41.7**	**42.56**	**2.06**
Ce, Fe	Reduction	488	15.7	28.4	1.8	**28.4**	**29.27**	**3.06**
Ce, Fe	As grown	488	11.3	20.6	1.0	**22.2**	**22.14**	**0.27**
Ce, Fe	Oxidation	488	1.6	18.8	0.8	**9.8**	**9.42**	**3.87**
Ce, Fe	Heavy Reduction	488	39.0	44.8	4.4	**38.6**	**39.79**	**3.08**
Ce, Fe	Reduction	514.5	16.2	30.5	1.9	**39.7**	**37.74**	**4.94**
Ce, Fe	Reduction	632.8	0.7	8.7	0.1	**27.8**	**28.41**	**2.19**

4. Conclusions

In conclusion, the theoretical analysis of the vectorial two-beam coupling in a photorefractive material has been presented and the related software tool has been developed, its use being important for design purposes. An example of its application has been presented in the case of a doped lithium niobate crystal, showing both the dependence of the conversion efficiency and signal gain on the crossing angle and the very different behaviour of the two (ordinary and extraordinary) polarizations. Comparisons between our numerical and experimentally measured coupling gain coefficients have been performed under a number of different technological conditions, showing high accuracy of our numerical predictions.

#1761 - $15.00 US Received October 21, 2002; Revised November 15, 2002